Desalination and Water Treatment
www.deswater.com

doi: 10.5004/dwt.2022.28946

276 (2022) 104–115
November

Using electro-peroxone process for petrochemical wastewater treatment: cost evaluation and statistical analysis

Safoora Karimi[a], Aref Shokri[b,c,*], Ali Hassani Joshaghani[d], Meisam Abdolkarimi-Mahabadi[c]

[a]*Department of Chemical Engineering, Jundi-Shapur University of Technology, Dezful, 334-64615 Iran*
[b]*Jundi-Shapur Research Institute, Jundi-Shapur University of Technology, Dezful, Iran, email: aref.shokri3@gmail.com*
[c]*Department of Chemical Engineering, Tafresh University, Tafresh 3951879611, Iran*
[d]*Department of Chemical Engineering, Faculty of Technical Engineering, Arak Branch, Islamic Azad University, Arak, Iran*

Received 16 May 2022; Accepted 25 September 2022

ABSTRACT

Recently, advanced oxidation processes (AOPs) are getting growing courtesy to be employed for petrochemical wastewater remediation. Electro-peroxone is a branch of AOPs which is a combination of ozone and electrochemically generated H_2O_2 that can generate hydroxyl radicals. In this study, it was used for the treatment of petrochemical wastewater. The central composite design (CCD), was utilized to investigate the impact of functional parameters on chemical oxygen demand (COD) removal (response). The optimal conditions predicted through the CCD were pH at 8.2, and the amount of COD at 1,340 mg/L, ozone flow rate at 1.00 L/min, and applied current at 1.61 Å. The graphical Pareto chart was executed to study the effect of each operative variable on the response and the amounts of COD have a remarkable impact on the removal of COD. The predicted and actual COD removal were 93.1% and 94%, respectively, at the predicted optimum conditions. The operational H_2O_2 generation from ozone at the cathode is the crucial parameter for the significant COD removal. The amounts of other parameters such as total organic carbon, total dissolved solids, and biological oxygen demand were reduced significantly. At optimal conditions, the COD was decreased from 1.34 to 0.11 kg/m^3 and the total reduction of COD was 1.23 kg/m^3. Due to the cost analysis, the operational cost was achieved to be 1.0 US $/m^3, and about 1.0 US $ was needed to treat 1 m^3 of studied wastewater. Therefore, this treatment method is more cost-effective.

Keywords: Electro-peroxone process; Pareto chart; Central composite design; Advanced oxidation processes

1. Introduction

The worldwide advance of pollution of water incomes together with evolving of various types of refractory contaminants enhanced serious global challenges. Nowadays, novel methods comprising photo electrocatalytic [1], photocatalysis [2], nano-filtration [3], electrocoagulation [4], peroxone [5], and photo-electro Fenton [6] have been employed in the common wastewater remediation which is somewhat weak in the degradation of pollutant molecules.

Moreover, to remediate resistant pollutants, ozonation investigations have been utilized [7]. Since ozone half-life in water is transient, it decays to O_2 only after its generation in a typical ozone process, which needs on-site generation and can result in significant expense. Also, ozone is selective for various chemical elements and various contaminants are resistant to it. As a result, ozone has been employed in addition to other advanced oxidation processes (AOPs), containing H_2O_2 [8] and electrolysis [9] to improve the effectiveness of pollutant degradation and

* Corresponding author.

surpass the challenges. Compared to the aforementioned approaches separately, the combination of ozone and the electrocatalytic oxidation methods can degrade contaminants since the producers convert only insignificant quantities of oxygen to ozone, which in turn leads to vast amounts of waste in oxygen and power consumption, as a result creating some challenges in ozone utilization. The peroxone approach, including H_2O_2 and ozone, has a combined effect on the pollutant treatment [10]. Nevertheless, the peroxone technique is hazardous for practical scale requirements due to the increase of H_2O_2. In contrast to a traditional peroxone approach, the electro-peroxone method is a novel branch of the advanced oxidation process (AOPs) that electrochemically generates in-situ H_2O_2 with adaptable ratios.

In the E-peroxone technique, in order to produce H_2O_2 from O_2 in the mixture of ozone and oxygen, the carbon-dependent cathode is utilized. Some of the main advantages of this approach are appropriate, secure, and cost-effective. To produce the in-situ OH radicals and H_2O_2 by cathodic reaction in the electro-peroxone technique [Eq. (1)], the researchers stabilized carbon-dependent electrodes. Based on Eq. (2), the injected O_3 reacts with the produced H_2O_2, and in turn, causes the generation of hydroxyl radical as a potent oxidizing species [11]. As a result, due to the production of hydroxyl radicals, such a process is significantly better compared with the separate ozonation and electrolysis process [12].

$$2H^+ + O_2 + 2e^- \rightarrow H_2O_2 \quad (1)$$

$$H_2O_2 + O_3 \rightarrow O_2^{\bullet-} + OH^{\bullet} + O_2 + H^+ \quad (2)$$

For designing and optimizing experiments, different conventional methods have existed. Even though the full factorial design (FFD) method evaluates the interactions between parameters, it is expensive and tedious [13]. The response surface methodology (RSM) is a series of statistical and mathematical techniques which is utilized to advance a helpful connection between response and input parameters [14]. The most frequent and widely employed design categories of the RSM includes Box–Behnken, three-level factorial, and central composite design (CCD). Between those methods, the CCD is used to regulate the impact of the parameters on the responses and ultimately for the process optimization. The CCD method is employed for evaluating the impact of individual operating parameters and their interaction, parameters optimization, and designing experiments, with a considerable reduction in the experiment numbers [15].

In this study, the issues that need extra investigations before its effective application in wastewater treatment, along with the affecting variables in the process, are explored. Lastly, the electro-peroxone method as a novel branch of AOPs was used to treat real industrial wastewater. It is a hybrid method in which, simple ozonation and electrolysis, and mechanisms are employed for indirect and direct oxidation of the pollutant. The aim of the process was the production of free hydroxyl radicals, and to improve the efficacy. The current wastewater including a mixture of aliphatic and aromatic hydrocarbons was attained from one of the companies in the special economic zone in Iran and it was treated by the electro-peroxone method. The impact of pH, ozone flow rate, applied current, and initial chemical oxygen demand (COD) amounts on the removal of COD was investigated and optimized by a central composite design.

2. Material and methods

2.1. Materials and apparatus

In this research, all chemicals containing sodium hydroxide, sodium sulfate, potassium iodide, and sulfuric acid were analytical scores and provided by Merck Company. The samples were achieved through one of the subsection companies of special economic zone petrochemical in Iran in spring of 2020 and kept in a laboratory at 4°C. Double-distilled water was employed in all tests. Each test applied 1,000 mL of wastewater. Sodium hydroxide (98%) and sulfuric acid (96%) were acquired from Merck Company and used for the adjustment of the initial pH.

The total organic carbon (TOC) was checked with an automatic autosampler Shimadzu TOC-VCSN providing and platinum-based catalyst. The synthetic air at the rate of 0.15 L/min was used as a carrier gas. The samples were acidified to lower than 4, before injecting the sample into the TOC analyzer, it was acidified with Phosphoric acid to persuade the inorganic carbon as CO_2 from the sample solution. The COD was determined by the HACH's COD technique by a COD reactor and a monitored by spectrophotometer (DR, 5000U) directly from the HACH Company.

The pH meter was from HACH Company and used for measuring pH. The DC source from ADAK Company (50 V, 5.00 Å, P405) was used. Before the test, some impurities of the wastewater were eliminated by filter paper after sedimentation, to avoid the reactor from choking.

2.2. Experimental design

As shown in Fig. 1, the wastewater with a particular COD was evaluated in a laboratory batch reactor. For the production of O_3 from a capsule comprising O_2 (99.9%), an O_3 producer from ARDA Company in Iran was employed. By altering the ozone producer power, the concentration of O_3 in the output of the O_3 producer (ozone and oxygen blend) can be attuned. Thus, the ozone producer release with a certain flow rate was passed to the bottom of the reactor by a fine sparger. The treatment process has occurred in galvanostatic settings through a DC power source. The carbon-polytetrafluorethylene (PTFE) cathode electrode and the anode were platinum sheets. Based on the high likelihood of H_2 evolution and their slight catalytic activity for degradation of H_2O_2, the electrodes of carbon-PTFE can change the O_3 to H_2O_2. Nevertheless, the metal electrodes might degrade H_2O_2 catalytically and hence cannot generate H_2O_2 from O_2 [16].

The distance between the anode and cathode was 3.0 cm, and the sufficient area of electrodes was 30 cm^2. The solution of Na_2SO_4 was utilized as a supplementary electrolyte,

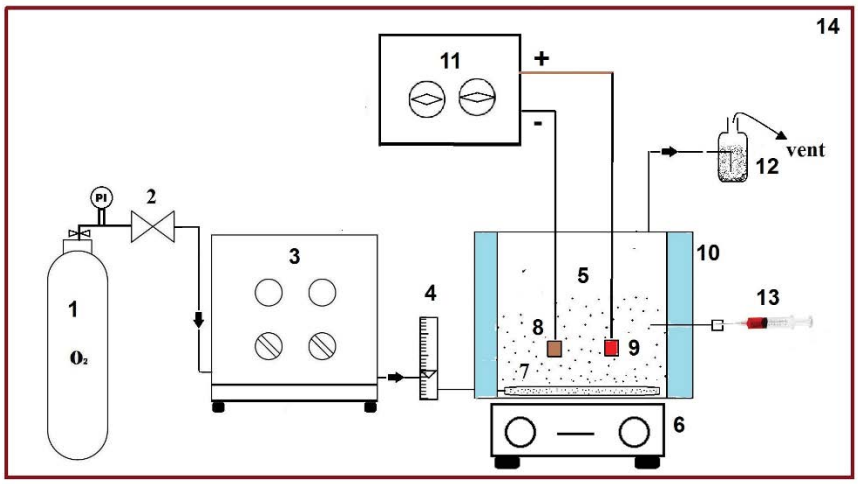

Fig. 1. The laboratory experimental set-up: 1- capsule of oxygen, 2- regulating valve, 3- ozone generation package, 4- flow meter, 5- reactor, 6- magnetic stirrer, 7- diffuser, 8- cathode electrode, 9- anode electrode, 10- jacket of water, 11- direct current supply, 12- destruction of O_3 destructor (KI solution, 2 wt.%), 13- specimen system, 14- wooden box [18].

and it didn't take into account the conductivity before treatment (Table 5). In the electro-peroxone technique, the DC power source and O_3 producer were initiated concurrently. By putting the reactor in a water bath which is governed by the circulation of water through a thermostat, the temperature was set at 25°C in all runs. The ozone concentration in the O_3 producer output was calculated based on the earlier investigation, and it was compatible with the ozone flow rate [17]. The reactor solution magnetically was unsettled. The first pH was adapted through H_2SO_4 (1 M) and NaOH addition and calculated through a basic pH Meter, PT-10P Sartorius Instrument Germany Company.

2.3. Analytical process

For each run, about 1,000 mL of industrial wastewater was experienced. Before each run, some scums were eliminated by filter paper and sedimentation to forbid the reactor from obstruction. The Samples were withdrawn, and after treatment, their COD was calculated based on the standard method by a UV-Vis spectrophotometer (American, Agilent, 5453) at 620 nm. The process response was COD removal (X_d) and achieved by Eq. (3). Moreover, depending upon the standard approach, the COD was ascertained, and the COD removal was achieved through Eq. (3):

$$X_d(\%) = \left(\frac{(\mathrm{COD})_0 - (\mathrm{COD})}{(\mathrm{COD})_0}\right) \times 100 \tag{3}$$

where (COD) and $(COD)_0$ are the amounts of COD at time t and the beginning of the reaction, respectively.

The electrostatic resistance between ions, electrodes, and ion exchange raised by electrolytes heightens the effectiveness of the approach comprising the oxygen reduction to H_2O_2 at the surface of the cathode. Based on the prior investigation, around 0.1 M of Na_2SO_4 was considered an electrolyte and it was constant in all tests.

Table 1
Scopes of the independent parameters

Variable	Levels				
	–2	–1	0	+1	+2
Initial COD (mg/L)	600	1,200	1,800	2,400	3,000
pH	4.5	6	7.5	9	10.5
Applied current (Å)	0.45	0.9	1.35	1.8	2.25
Flow rate of O3 (L/min)	0.3	0.6	0.9	1.2	1.5

2.4. Experimental setup

In order to explore the impact of pH, initial concentration of dye (C_{D0}), the ozone flow rate, and applied current (Å) on COD removal, the CCD method was utilized. The scope of input parameters, as shown in Table 1 at both natural and coded amounts were chosen to cover a viable scope of parameters. The stock solution of wastewater has a COD of 3,000 mg/L and in Table 1, different level of initial COD was prepared by dilution with distilled water.

The CCD included factorial points (n_F = 16 runs) from an FFD design, with a replicated central point (n_C = 7 runs), and axial points (n_A = 8 runs). A value of $\alpha = (n_F)^{1/4} = 2$ was reserved for the design to be rotatable [19].

The design of regression is used for modeling response as a mathematical model. The experiment parameters are coded to improve the regression equation as Eq. (4):

$$x_i = \frac{X_i - X_i^x}{\Delta X_i} \tag{4}$$

where x_i and X_i are the coded and real amounts of the ith independent element; respectively, the step change value is ΔX_i and X_i^x is the ith independent coded variable at the center point. So, the subsequent dimensionless equation was obtained:

$$x_1 = A = \frac{C_{D_0} - 700}{200},\ x_2 = B = \frac{\text{ph} - 6.5}{1.5},$$
$$x_3 = C = \frac{AC - 0.6}{0.2},\ x_4 = D = \frac{O_3 - 0.9}{0.3} \quad (5)$$

To assess the accuracy of the model and calculate the test error, the replicates were utilized. Normally, it was clear from Table 2, that the experimental design comprises 30 runs, which are conducted in an accidental order to decrease the effects of flexibility in the response due to unnecessary factors.

3. Results and discussions

The investigation of outcomes was obtained through the Statistical software, Design-Expert 10, (Minneapolis, MN, Stat-Ease Incorporation) in the USA. The following model [Eq. (6)] which is a polynomial equation was recommended for the response (Y) and the outcomes are demonstrated in Table 2 [20].

$$Y = \beta_0 + \sum_{i=1}^{4}\beta_i x_i + \sum_{i=1}^{4}\beta_{ii} x_i^2 + \sum_{i=1}^{4}\sum_{j=1,i<j}^{4}\beta_{ij} x_i x_j \quad (6)$$

where x_i is the coded independent variables and Y is the response, the intercept is b_{ii}, b_{ij}, b_i, and β_0 are the quadratic regression, pure interaction, and linear coefficients, respectively. Because of the proper interpolation ability and simple calculation of variables, typically, polynomial models are utilized to elucidate complicated designs.

The achieved information must be statistically investigated utilizing regression if there is an association between the parameters and response.

3.1. Results of analysis of variance

To optimize and explore the influence of the functional variables on the COD removal efficacy, the RSM was utilized. The analysis of variance (ANOVA) was utilized to obtain the contact between the parameters and response, which is shown in Table 3. The *F*-value indicates the

Table 2
Planning of tests with their elements and corresponding response (COD removal)

Std.	Factor 1	Factor 2	Factor 3	Factor 4	Response
	A: initial COD, (mg/L)	*B*: pH	*C*: applied current, (Å)	*D*: O_3 flow rate, (L/min)	COD removal (%)
1	1,200	6	0.9	0.6	73
2	2,400	6	0.9	0.6	46
3	1,200	9	0.9	0.6	85
4	2,400	9	0.9	0.6	54
5	1,200	6	1.8	0.6	68
6	2,400	6	1.8	0.6	44
7	1,200	9	1.8	0.6	87
8	2,400	9	1.8	0.6	60
9	1,200	6	0.9	1.2	77
10	2,400	6	0.9	1.2	55
11	1,200	9	0.9	1.2	92
12	2,400	9	0.9	1.2	66
13	1,200	6	1.8	1.2	70
14	2,400	6	1.8	1.2	51
15	1,200	9	1.8	1.2	94
16	2,400	9	1.8	1.2	71
17	600	7.5	1.35	0.9	87
18	3,000	7.5	1.35	0.9	37
19	1,800	4.5	1.35	0.9	50
20	1,800	10.5	1.35	0.9	81
21	1,800	7.5	0.45	0.9	80
22	1,800	7.5	2.25	0.9	80
23	1,800	7.5	1.35	0.3	58
24	1,800	7.5	1.35	1.5	73
25	1,800	7.5	1.35	0.9	84
26	1,800	7.5	1.35	0.9	85
27	1,800	7.5	1.35	0.9	84
28	1,800	7.5	1.35	0.9	84
29	1,800	7.5	1.35	0.9	85
30	1,800	7.5	1.35	0.9	84

Table 3
Results of ANOVA in the removal of COD by the electro-peroxone method

Source	Sum of squares	DF	Mean square	*F*-value	*p*-value	
Model	7,196.22	14	514.02	4,688.86	<0.0001	Significant
A-COD	3,655.60	1	3,655.60	33,346.42	<0.0001	
B-pH	1,422.96	1	1,422.96	12,980.25	<0.0001	
C-applied current	0.4874	1	0.4874	4.45	0.0522	
D-ozone flow rate	316.83	1	316.83	2,890.10	<0.0001	
AB	16.00	1	16.00	145.95	<0.0001	
AC	10.56	1	10.56	96.35	<0.0001	
AD	23.52	1	23.52	214.57	<0.0001	
BC	74.82	1	74.82	682.53	<0.0001	
BD	16.40	1	16.40	149.62	<0.0001	
CD	0.6400	1	0.6400	5.84	0.0289	
A^2	856.26	1	856.26	7,810.81	<0.0001	
B^2	618.80	1	618.80	5,644.72	<0.0001	
C^2	28.88	1	28.88	263.40	<0.0001	
D^2	635.20	1	635.20	5,794.25	<0.0001	
Residual	1.64	15	0.1096			
Lack of fit	0.6310	10	0.0631	0.3114	0.9451	Not significant
Pure error	1.01	5	0.2027			
Cor. total	7,197.87	29				

statistical consequence of the model, and the *p*-value was fixed at 0.05. The *p*-value will be much decreased when the *F*-value is lower than the estimated *F*-value, it represents the importance of the statistical model. The *F*-value of 4688.86 recommends that the model is significant vs. noise. Such a significant *F*-value can be due to noise just with a 0.01% probability [21].

The model terms are important if the *p*-values are less than 0.0500. In this research, the terms *A*, *B*, *D*, *C*, *CD*, *AB*, *BD*, *AC*, B^2, A^2, and C^2 are significant. Nevertheless, the *p*-value of linear *CD*, *BD*, and *AD* was greater than 0.05; as a result, the suggested relations appear to be insignificant variables. On the contrary, the values superior to 0.1000 indicate that the model terms are insignificant.

As demonstrated in Table 3, to enhance the model, the insignificant terms were removed. Since in the lack of fit, the *F*-value was 0.3114, the lack of fit is insignificant; as a result, there is a 94.51% chance that it was due to noise. The *p*-value for lack of fit was more than 0.05 and recommends that it is insignificant so the lack of fit is in the proper range and the model fitness is probable.

The *F*-value, adjusted R^2 between the experimental, coefficient of determination (R^2), predicted values, and the sum of squares value, was utilized to evaluate the statistical importance of the model. The R^2 was 0.9998, and the adjusted R^2 of 0.9996 was in accurate agreement with the predicted R^2 at 0.9993.

Moreover, in the assessment to determine if a variable is significant or not, the sum of squares must be explored. The significance of parameters and the sum of squares are directly proportional [22]. Based on the outcomes, the second-order polynomial predicted response is consequent as the resulting Eq. (7):

$$\begin{aligned}\text{COD Removal}(\%) = {} & 84.27 + 12.34A + 7.7B - 0.1425C \\ & + 3.63D - 1.0000AB + 0.8125AC \\ & + 1.21AD + 2.16BC + 1.01BD \\ & - 0.200CD - 5.59A^2 - 4.75B^2 \\ & - 1.03C^2 - 4.81D^2 \end{aligned} \quad (7)$$

The predicted equation for the response, which was dependent upon actual variables, can be utilized for specific ranges of each factor. The ranges of each variable must be reported in the original unit. Since the coefficients are scaled to adapt each factor unit, and the center of the design space does not have the intercept and the comparative effect of each factor cannot be determined through this equation [23].

3.2. Effect of current intensity

The 3-dimensional surface and contour plots were utilized to demonstrate the interactions between factors, and in Fig. 2 the influence of applied current on COD removal is shown. One of the factors that significantly could enhance the effectiveness of the electro-peroxone technique is the appropriate intensification of the selected functional parameters. Although a further rise in current to 1.4 Å does not have more influence, an upsurge in current intensity from 0.4 to 1.4 Å can improve the COD removal insignificantly. At significant levels of current intensity, a considerable number of H_2O_2 molecules and, as a result, OH radicals were generated, which can interact with H_2O_2 to create a weak oxidative agent (hydro peroxyl) as compared to OH radicals or scavenge each other at great concentration.

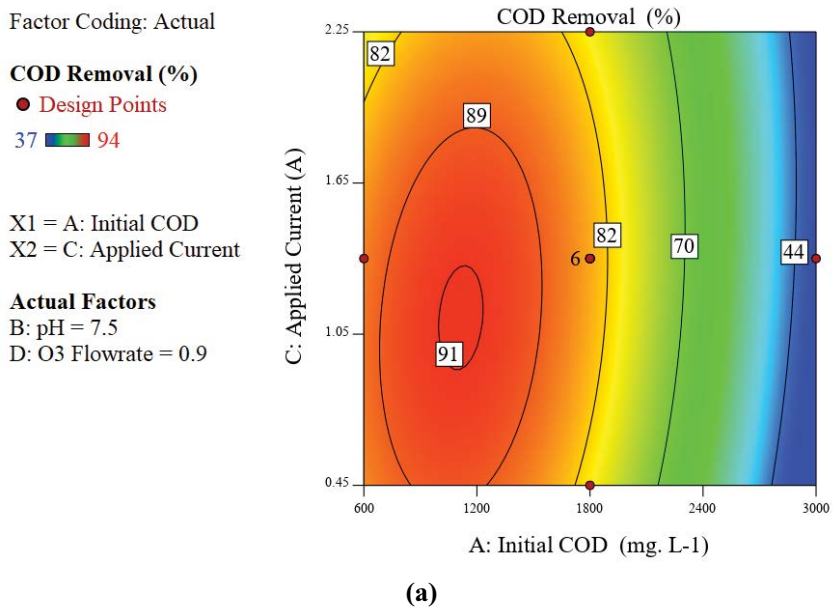

(a)

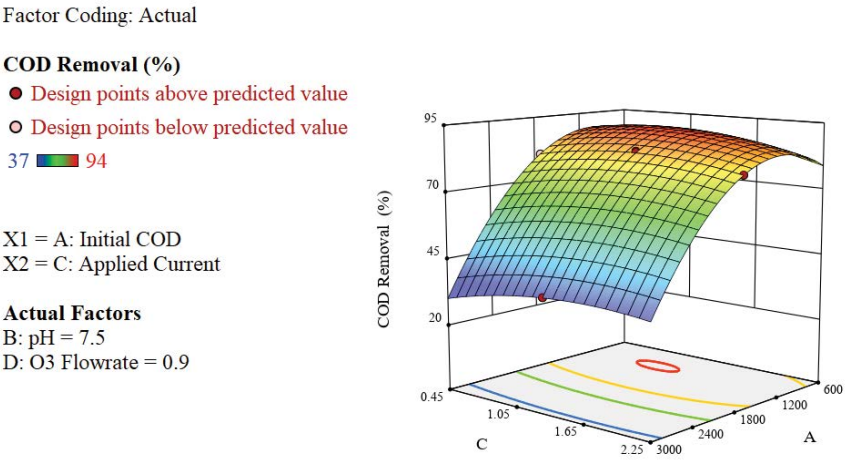

(b)

Fig. 2. Impact of current intensity on the removal of COD after 60 min of remediation reaction; (a) contour plot and (b) response surface plot.

Additional advance in current intensity has a negligible influence on the effectiveness of the treatment process and in such conditions, since the ozone dissolution ratio in water was slight, and extra H_2O_2 interacted with hydroxyl radicals, the hydroxyl radical production was saturated. Moreover, because H_2O_2 can be decreased instead of O_3 at the cathode surface, the H_2O_2 decayed at the cathode surface at a high applied current [24]. As a result, the effectiveness of the electro-peroxone method does not enhance at an extreme raised current. In addition, Zheng et al. [25] accidentally discovered the same phenomenon. The additional H_2O_2 can interact with hydroxyl radicals as a scavenger [Eqs. (8) and (9)], or it can decrease and decay H_2O_2, hence decreasing the electro-peroxone method's effectiveness [26].

$$H_2O_2 + OH^{\bullet} \rightarrow HO_2^{\bullet} + H_2O \quad (8)$$

$$HO_2^- + H_2O + 2e^- \rightarrow 3OH^- \quad (9)$$

Furthermore, the anodic oxidations and cathodic reductions (O_3 and O_2 reductions) were accelerated with an increase in applied current which would generate additional reactive oxygen species (ROS).

3.3. Influence of ozone flow rate

It is worth mentioning that both ozone relevant flow rate and its concentration at the output of ozone producer are essential. Depending upon the initial experimental results, at a certain ozone producer power, the inlet O_3 concentration was reduced with an advance in the flow rate of inputted pure O_2. To establish the ozone concentration at the exhaust gas, at various ozone flow rates the

power of the O_2 producer was changed. Although in the electro-peroxone process, the calculation of ozone concentration in the liquid phase was complicated, it is regarded as an essential parameter. As a result, since at a certain amount of pure oxygen flow rate and adaptable power of ozone producer, the ozone concentration in the liquid phase can be relevant to the ozone flow rate; in this investigation, the outlet flow rate of ozone producer was explored. Such results are defined totally in our prior research [27]. Through an upsurge in the oxygen flow rate, the transformation of O_3 from the gas to the aqueous phase was improved. Hence, the ozone interactions with H_2O_2 and the ozone decrease at the cathode surface were raised. With an upsurge in the O_3 flow rate, the reaction between ozone and H_2O_2 was raised and ultimately caused the production of more hydroxyl radicals, which enhanced the efficiency of pollutant removal (Fig. 3).

Moreover, based on the increased mass transfer of O_3 from gas to liquid phase, a rise in the concentration of O_3 in the inlet gas phase could supply the peroxone and ozonation interactions, depending upon the mass transformation rule [28]. The ozone concentration in a liquid phase is significantly crucial in the reaction of pollutants with O_3 in aqueous surroundings, and it was an indicator for the number of entered O_3 into the solution at an explicit time, the volume, and temperature of a liquid in the reactor.

The COD removal was enhanced by increasing the ozone flow rate in the sparged gas and then enhanced the mass transfer of O_3 from gas to a liquid phase. As a result, more OH radicals can be generated from cathodic reduction

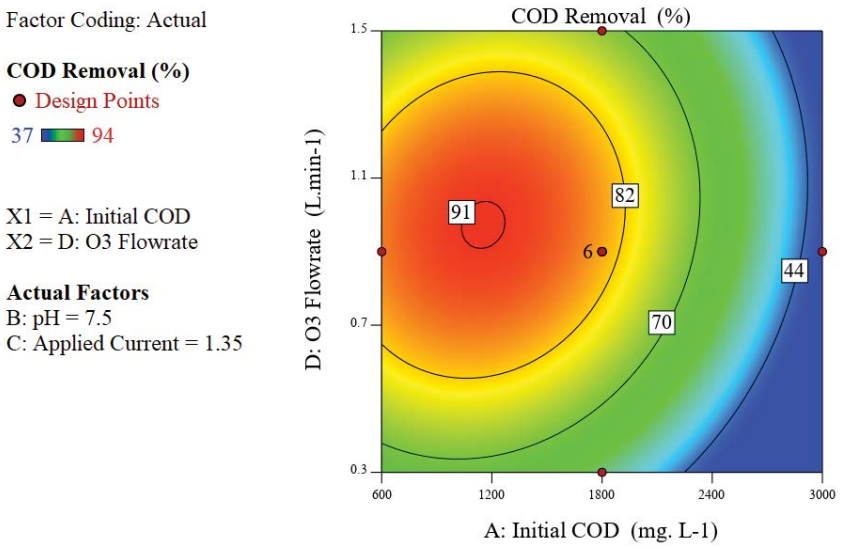

(a)

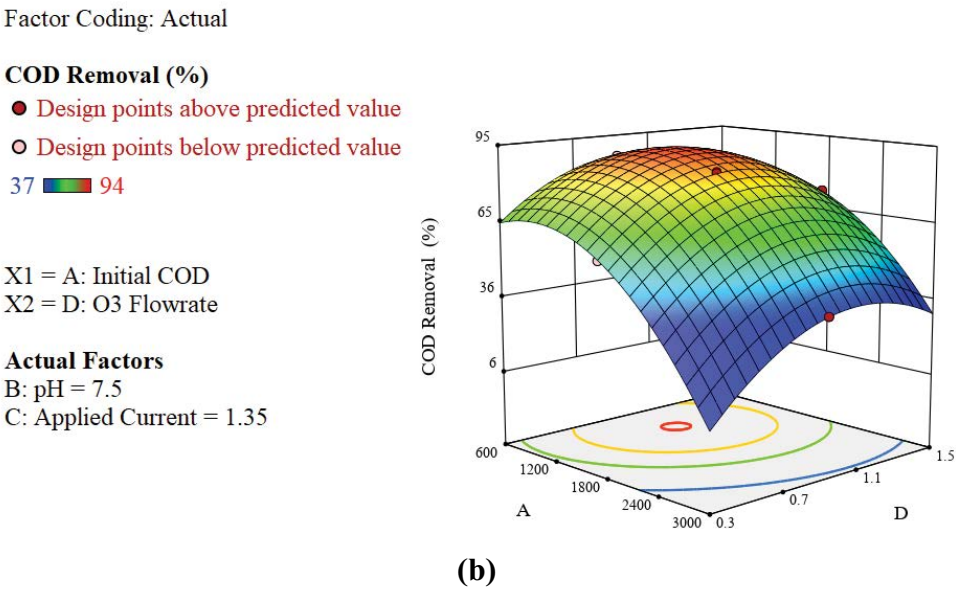

(b)

Fig. 3. Impact of ozone flow rate on the COD removal after 60 min of remediation; (a) contour plot and (b) response surface design.

between O_3 and H_2O_2, which causes enhanced levels of COD removal in the electro-peroxone process. Nevertheless, great ozone flow rates might have little impact on the pollutant removal effectiveness because of the O_3 discharge from the liquid phase and scavenging impacts of generated hydroxyl radicals and ozone molecules. Moreover, such results were approved by Wu et al. [29].

3.4. Effect of initial pH

Through using HCl (0.1 M) and NaOH, the pH was adjusted, and because of the generation of the acidic intermediate throughout the interaction, it was not calculated and decreased a bit. The influence of initial pH on the COD removal was investigated, and the outcomes are shown in Fig. 4. Typically, the ozonation method performs well enough in primary pH because the interaction of ozone with hydroxide ions causes the formation of HO_2^- which interacts with O_3 and form hydroxyl radicals [Eqs. (10) and (11)]. Moreover, such interactions occurred in alkaline situations through the electro-peroxone process. Nevertheless, H_2O_2 can scavenge the soluble O_3 and reduce the generated OH radical [30].

$$OH^- + O_3 \rightarrow HO_2^- + O_2 \quad (10)$$

$$HO_2^- + O_3 \rightarrow O_2 + O_2^{\bullet -} + OH^{\bullet} \quad (11)$$

Another possible process is that the conjugated H_2O_2 or the basic form of hydrogen peroxide interacts with O_3

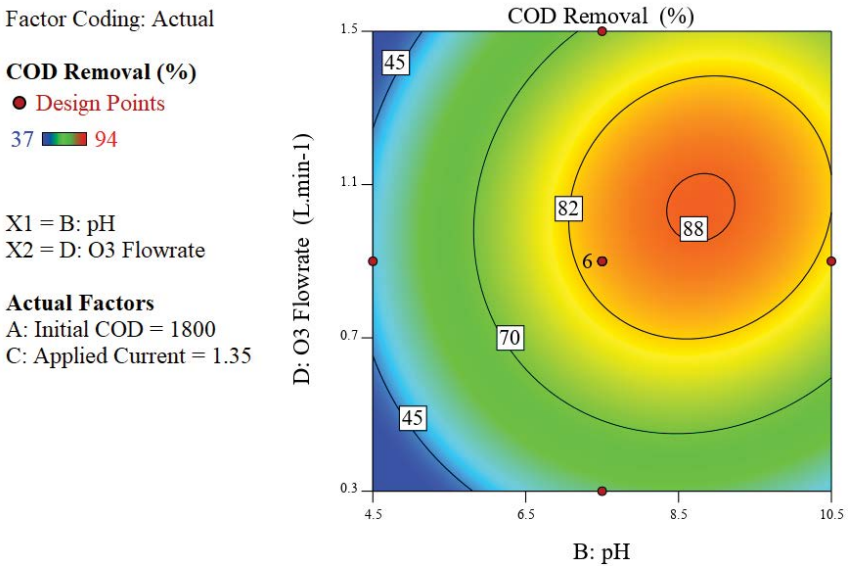

(a)

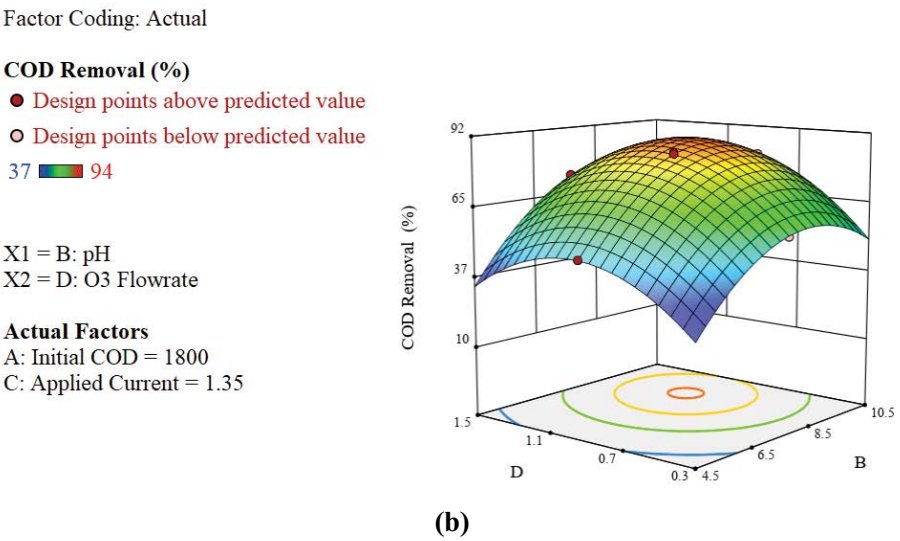

(b)

Fig. 4. Impact of pH on the COD removal after 60 min of remediation; (a) contour plot and (b) response surface plot.

to generate OH radicals [Eq. (12)] to interact with contaminants in an aqueous mixture [31].

$$2HO_2^- + H_2O + 2O_3 \rightarrow 2OH^- + HO_2^{\bullet} + 3O_2 + OH^{\bullet} \quad (12)$$

In acidic environments, the perfect efficacy of the electro-peroxone method might be due to the better effectiveness of electrodes in H_2O_2 generation. While the remediation process might vary at different levels of pH, nevertheless, depending on the outcomes, the pollutant removal efficiency was high enough in more acidic or alkaline environments, and such complication is admitted by other investigators [32]. In general, the alkaline environment was feasible in the electro-peroxone method [33]; but, the high values of pH reduce the COD removal effectiveness due to the low electro-production of H_2O_2 motivated by the low dosage of the proton [Eq. (1)].

3.5. Influence of initial COD

The amounts of initial COD and the time for COD removal are inversely correlated together, as was obvious from the empirical analyses (Fig. 5). Certain amounts of oxidizing

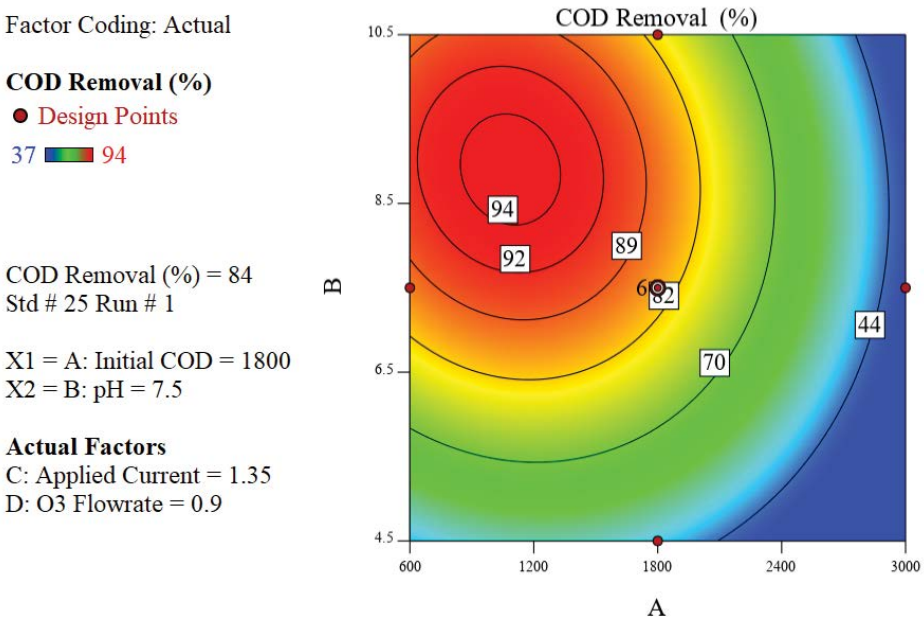

(a)

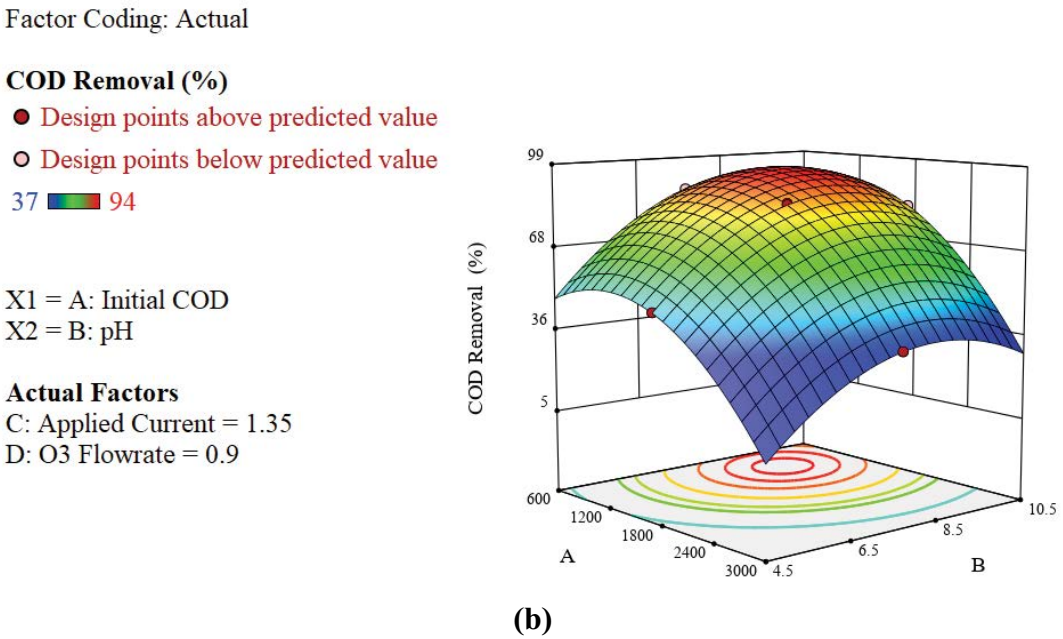

(b)

Fig. 5. Impact of initial COD on the COD removal after 60 min of remediation; (a) contour plot and (b) response surface design.

species were generated in the electro-peroxone method, raising the COD amounts, which caused the progress in reaction time or decrease in degradation effectiveness. Based on the given concentration of oxidation species in electrochemical approaches, the power utilization can be enhanced somewhat through an enhancement in the contaminant concentration because of the increase in the reaction chance between the contaminant molecules and oxidizing agent (frequently OH radicals). Such tendency remains until the generated side-products hinder the removal effectiveness [34].

3.6. Pareto charts

In order to judge the coincident impacts of different parameters, and as a result, seek the optimum situations for appropriate responses, the RSM is an effective statistical-dependent approach. The crucial parameters that influence the response can be detected by considering the Pareto chart. The effects of experiential factors on the response at optimal situations in contour plots (Figs. 2–5) and 3-dimensional response surfaces were depicted through Pareto graphs (Fig. 6). As the parameters were attained, detecting the remarkable impacts at 95% confidence and both of the major impacts and their reaction are demonstrated.

The Pareto chart graph is performed to show the impact of each functional parameter on the response and evaluated through the below equivalence Eq. (13) [20].

$$P_i = \left(\frac{b_i^2}{\sum b_i^2} \right) \times 100 \tag{13}$$

The term bi indicates the numerical coefficient effect for each parameter. The pH and amounts of initial COD were the essential parameters that significantly influenced the COD removal. Due to the residual contributions, in the process the effect of the applied current was little

3.7. Operational condition optimization

The COD removal effectiveness was significant in certain situations, and the quantities of different variables were optimized through design expert software. The amounts of different parameters in the removal of COD are demonstrated in Table 4.

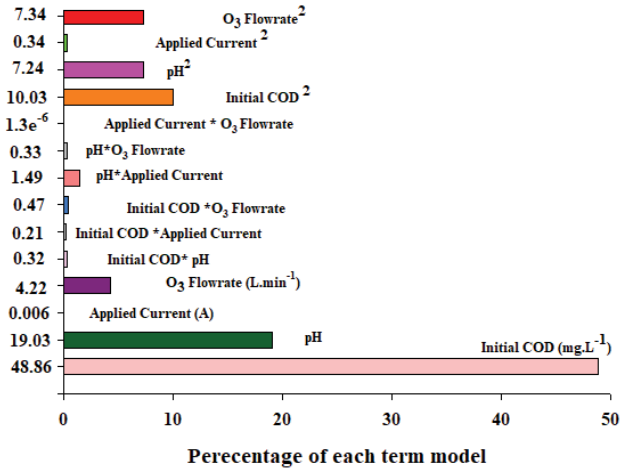

Fig. 6. Graphical Pareto for the parameters in COD removal.

The optimal conditions predicted through the CCD were; the initial amount of COD at 1,340 mg/L, ozone flow rate at 1.00 L/min, pH at 8.2, and applied current at 1.61 Å. The experiment was repeated one more time at the predicted optimal situations, and COD removal was 93.1%. In this research, 60 min of treatment was selected in all runs to investigate any possible changes appropriately. The COD quantity was reduced from 1,340 to 110 mg/L, as a result, the COD was degraded significantly; nevertheless, the generated intermediates had COD. The predicted COD removal was 93.1% which was suggested by the software. The real wastewater after dilution with distilled water to produce achieved optimum initial COD has the following features (Table 5), including total dissolved solids (TDS), biological oxygen demand (BOD), COD, TOC, pH, and conductivity.

The outcomes stated above confirmed the prior investigations. The H_2O_2 is considered a weak oxidant [35]. Although ozone can oxidize organics breaking double bonds quickly [36]. Typically, the hydroxyl radical has an essential function in the conventional electro-peroxone approach.

3.8. Cost evaluation

The current study is on a laboratory scale, but on an industrial scale, the cost evaluation includes some factors such as electricity, equipment installation, disposal of electrolytes sludge, and maintenance of labor, and plant. But, due to Eq. (14), the operating cost in the mentioned process was

Table 4
Optimal conditions in the COD removal

Variables	Value
Applied current, At	1.61
pH	8.2
Ozone flow rate, L/min	1.00
Initial COD, mg/L	1340
Predicted COD removal, %	93.10
Experimental COD removal, %	94.0

Table 5
Features of wastewater in an industrial company

Property	Results	
	Before electro-peroxone	After electro-peroxone
TDS, ppm	2,600	1,100
TOC, ppm	1,000	300
BOD_5, ppm	500	100
COD, ppm	1,340	80
pH	8.0	7.0
Conductivity, μS/cm	3,000	1,200

calculated using three key factors that are electrical energy consumption, electrode consumption, and electrolyte consumption as chemicals [37,38].

$$\text{Operation Cost} = a\left(E_T\right) + b\left(E_C\right) + C\left(C_C\right) \quad (14)$$

where E_C is electrode consumption in kg/m^3, E_T is total electrical consumption in KWh/m^3, and C_C is chemical consumption in kg/m^3. The total electrical consumption can be calculated by Eq. (1). Moreover, *a*, *b* and *c* are the unit price of consumed electricity, electrode material; and electrolyte (Na_2SO_4), respectively. At the optimal operational condition for the electro-peroxone process, the electrical energy was calculated to be 2.2 kWh/m^3. The chemical consumptions were about 0.4 kg/m^3, but in this study due to the conductance of the real sample (Table 1) the addition of electrolytes was negligible.

The analysis of cost can be done as per unit COD. At optimal conditions, the COD was decreased from 1.34 to 0.11 kg/m^3 and the total reduction of COD was 1.23 kg/m^3. Approximately, the valued operational cost was achieved to be 1.0 US $/m^3. Therefore, the cost per unit COD reduction was 0.812 $/COD drop. The treatment cost depends on the pollutants type and their concentration.

The electro-peroxone process can compete with other methods. But the process cost depends on the organic load. In terms of fixed capital cost, it needs more costly compared to electrocoagulation and coagulation. In addition, the pollutant removal efficacy is higher whereas labor, maintenance, sludge disposal, and transportation cost are low. These statements are in agreement with the results of other researchers [39].

4. Conclusions

In this study, the COD removal in the wastewater of an Iranian petrochemical company was explored through the E-peroxone approach as a combination of electrochemically produced hydrogen peroxide and ozone which can generate potent OH radicals. The CCD was employed to evaluate the influence of functional parameters on the COD removal. The optimum situations predicted by the CCD were; pH at 8.2, the ozone flow rate at 1.00 L/min, and COD concentration at 1,340 mg/L and applied current at 1.61 Å. The Pareto chart demonstrated that the amounts of COD have a considerable effect on the response.

Based on the significant COD removal (around 94%) at a low time, it can be understood that the E-peroxone approach cannot generate secondary pollutants. As a result, it is an eco-friendly wastewater remediation method. For the broad use of the electro-peroxone technique, optimizing reactor configurations and applied variables to increase the mass transfer of O_2 and later substantial current efficiency for electrically generated H_2O_2 is important.

A considerable synergy for the removal of COD through the electro-peroxone can be relevant to different processes comprising the ozone electro-reduction to OH ion close to the cathode

The cost analysis was performed and about 1.0 US$ was needed to treat 1 m^3 of studied wastewater. Therefore, in view of cost-effectiveness, this treatment method is more satisfactory.

References

[1] J. Sun, H. Maimaiti, B. Xu, L. Feng, J. Bao, X. Zhao, Photoelectrocatalytic degradation of wastewater and simultaneous hydrogen production on copper nanorod-supported coal-based N-carbon dot composite nanocatalysts, Appl. Surf. Sci., 585 (2022) 152701, doi: 10.1016/j.apsusc.2022.152701.

[2] A. Shokri, K. Mahanpoor, Using UV/ZnO process for degradation of Acid red 283 in synthetic wastewater, Bulg. Chem. Commun., 50 (2018) 27–32.

[3] G. Abdi, A. Alizadeh, S. Zinadini, G. Moradi, Removal of dye and heavy metal ion using a novel synthetic polyethersulfone nanofiltration membrane modified by magnetic graphene oxide/metformin hybrid, J. Membr. Sci., 552 (2018) 326–335.

[4] A. Shokri, Employing electrocoagulation for the removal of Acid Red 182 in aqueous environment by using Box–Behenken design method, Desal. Water Treat., 115 (2018) 281–287.

[5] M. Cashman, R. Ball, T. Lewis, T.B. Boving, Peroxone activated persulfate oxidation of 1,4-dioxane under column scale conditions, J. Contam. Hydrol., 245 (2022) 103937, doi: 10.1016/j.jconhyd.2021.103937.

[6] G. Divyapriya, R. Srinivasan, J. Mohanalakshmi, I.M. Nambi, Development of a hybrid bifunctional rotating drum electrode system for the enhanced oxidation of ciprofloxacin: an integrated photoelectrocatalysis and photo-electro-Fenton processes, J. Water Process Eng., 49(2022) 102967, doi: 10.1016/j.jwpe.2022.102967.

[7] S. Lim, J.L. Shi, U. Gunten, D.L. McCurry, Ozonation of organic compounds in water and wastewater: a critical review, Water Res., 213 (2022) 118053, doi: 10.1016/j.watres.2022.118053.

[8] O.M. Cornejo, J.L. Nava, Incineration of the antibiotic chloramphenicol by electro-peroxone using a smart electrolyzer that produces H_2O_2 through electrolytic O_2, Sep. Purif. Technol., 282 (2022) 120021, doi: 10.1016/j.seppur.2021.120021.

[9] S. Li, J. Huang, Y. Wang, G. Yu, Role of in-situ electrogenerated H_2O_2···bridge in tetracycline degradation governed by mechanochemical Si-O anchoring Cu^{2+} as electron shuttle during E-peroxone process, Appl. Catal., B, 304 (2022) 120930, doi: 10.1016/j.apcatb.2021.120930.

[10] H. Chen, J. Wang, Degradation and mineralization of ofloxacin by ozonation and peroxone (O_3/H_2O_2) process, Chemosphere, 269 (2021) 128775, doi: 10.1016/j.chemosphere.2020.128775.

[11] Y. Zhang, S. Zuo, Y. Zhang, M. Li, J. Cai, M. Zhou, Disinfection of simulated ballast water by a flow-through electro-peroxone process, Chem. Eng. J., 348 (2018) 485–493.

[12] J. Yao, B. Yu, H. Li, Y. Yang, Interfacial catalytic and mass transfer mechanisms of an electro-peroxone process for selective removal of multiple fluoroquinolones, Appl. Catal., B, 298 (2021) 120608, doi: 10.1016/j.apcatb.2021.120608.

[13] R. Khawaga, M. Abouleish, N.A. Jabbar, S. Al-Asheh, Chlorination breakpoint with nitrite in wastewater treatment: a full factorial design experiments, J. Environ. Chem. Eng., 9 (2021) 104903, doi: 10.1016/j.jece.2020.104903.

[14] A.I. Adeogun, P.B. Bhagawati, C.B. Shivayogimath, Pollutants removals and energy consumption in electrochemical cell for pulping processes wastewater treatment: artificial neural network, response surface methodology and kinetic studies, J. Environ. Manage., 281 (2021) 111897, doi: 10.1016/j.jenvman.2020.111897.

[15] R. Lessoued, L. Baameur, A. Tabchouche, Modeling and optimization of COD removal from leachate by electrocoagulation: application of central composite design, Environ. Model. Assess., 26 (2021) 423–432.

[16] O.M. Cornejo, J.L. Nava, Mineralization of the antibiotic levofloxacin by the electro-peroxone process using a filter-press flow cell with a 3D air-diffusion electrode, Sep. Purif. Technol., 254 (2021) 117661, doi: 10.1016/j.seppur.2020.117661.

[17] A. Shokri, Degradation of 2-nitrophenol from petrochemical wastewater by ozone, Russ. J. Appl. Chem., 88 (2015) 2038–2043.

[18] A. Shokri, S. Karimi, Treatment of aqueous solution containing Acid red 14 using an electro-peroxone process and a Box–Behnken experimental design, Arch. Hyg. Sci., 9 (2020) 48–57.
[19] I. Basturk, G. Varank, S. Murat-Hocaoglu, S. Yazici-Guvenc, E.E. Oktem-Olgun, O. Canli, Characterization and treatment of medical laboratory wastewater by ozonation: optimization of toxicity removal by central composite design, Ozone Sci. Eng., The J. Int. Ozone Assoc., 43 (2021) 213–227.
[20] A. Shokri, Employing electro-peroxone process for degradation of Acid Red 88 in aqueous environment by central composite design: a new kinetic study and energy consumption, Chemosphere, 296 (2022) 133817, doi: 10.1016/j.chemosphere.2022.133817.
[21] A. Shokri, A. Bayat, K. Mahanpoor, Employing Fenton-like process for the remediation of petrochemical wastewater through Box–Behnken design method, Desal. Water Treat., 166 (2019) 135–143.
[22] A. Shokri, Employing UV/peroxydisulphate (PDS) activated by ferrous ion for the removal of toluene in aqueous environment: electrical consumption and kinetic study, Int. J. Environ. Anal. Chem., (2020) 1–18, doi: 10.1080/03067319.2020.1784887.
[23] A. Shokri, Employing sono-Fenton process for degradation of 2-nitrophenol in aqueous environment using Box–Behnken design method and kinetic study, Russ. J. Phys. Chem. A, 93 (2019) 243–249.
[24] Z. Guo, Y. Xie, Y. Wang, H. Cao, J. Xiao, J. Yang, Y. Zhang, Towards a better understanding of the synergistic effect in the electro-peroxone process using a three electrode system, Chem. Eng. J., 337 (2018) 733–740.
[25] H.-S. Zheng, W.-Q. Guo, Q.-L. Wu, N.-Q. Ren, J.-S. Chang, Electro-peroxone pretreatment for enhanced simulated hospital wastewater treatment and antibiotic resistance genes reduction, Environ. Int., 115 (2018) 70–78.
[26] D. Wu, G. Lu, R. Zhang, Q. Lin, J. Yao, X. Shen, W. Wang, Effective degradation of diatrizoate by electro-peroxone process using ferrite/carbon nanotubes based gas diffusion cathode, Electrochim. Acta, 236 (2017) 297–306.
[27] A. Shokri, M. Sanavi Fard, Employing electro-peroxone process for industrial wastewater treatment: a critical review, Chem. Pap., 76 (2022) 5341–5367.
[28] B. Wang, W. Shi, H. Zhang, H. Ren, M. Xiong, Promoting the ozone-liquid mass transfer through external physical fields and their applications in wastewater treatment: a review, J. Environ. Chem. Eng., 9 (2021) 106115, doi: 10.1016/j.jece.2021.106115.
[29] D. Wu, G. Lu, J. Yao, C. Zhou, F. Liu, J. Liu, Adsorption and catalytic electro-peroxone degradation of fluconazole by magnetic copper ferrite/carbon nanotubes, Chem. Eng. J., 370 (2019) 409–419.
[30] G. Asgari, A. Seid-mohammadi, A. Rahmani, M.T. Samadi, M. Salari, S. Alizadeh, D. Nematollahi, Diuron degradation using three-dimensional electro-peroxone (3D/E-peroxone) process in the presence of TiO_2/GAC: application for real wastewater and optimization using RSM-CCD and ANN-GA approaches, Chemosphere, 266 (2021) 129179, doi: 10.1016/j.chemosphere.2020.129179.
[31] Q. Hu, H. Liu, Z. Zhang, Y. Xie, Nitrate removal from aqueous solution using polyaniline modified activated carbon: optimization and characterization, J. Mol. Liq., 309 (2020) 113057, doi: 10.1016/j.molliq.2020.113057.
[32] R. Srinivasan, I.M. Nambi, An electro-peroxone-based multi-pronged strategy for the treatment of ibuprofen and an emerging pharmaceutical wastewater using a novel graphene-coated nickel foam electrode, Chem. Eng. J., 450 (2022) 137618, doi: 10.1016/j.cej.2022.137618.
[33] M. Ghalebizade, B. Ayati, Acid Orange 7 treatment and fate by electro-peroxone process using novel electrode arrangement, Chemosphere, 235 (2019) 1007–1014.
[34] M. Ghalebizade, B. Ayati, Solar photoelectrocatalytic degradation of Acid Orange 7 with ZnO/TiO_2 nanocomposite coated on stainless steel electrode, Process Saf. Environ. Prot., 103 (2016) 192–202.
[35] B. Bakheet, S. Yuan, Z. Li, H. Wang, J. Zuo, S. Komarneni, Y. Wang, Electro-peroxone treatment of Orange II dye wastewater, Water Res., 47 (2013) 6234–6243.
[36] L. Kovalova, H. Siegrist, U. von Gunten, J. Eugster, M. Hagenbuch, A. Wittmer, R. Moser, C.S. McArdell, Elimination of micropollutants during post-treatment of hospital wastewater with powdered activated carbon, ozone, and UV, Environ. Sci. Technol., 47 (2013) 7899–7908.
[37] S. Sen, A.K. Prajapati, A. Bannatwala, D. Pal, Electrocoagulation treatment of industrial wastewater including textile dyeing effluent – a review, Desal. Water Treat., 161 (2019) 21–34.
[38] D. Sharma, P.K. Chaudhari, S. Dubey, A.K. Prajapati, Electrocoagulation treatment of electroplating wastewater: a review, J. Environ. Eng., 146 (2020) 03120009, doi: 10.1061/(ASCE)EE.1943-7870.0001790.
[39] A.K. Prajapati, P.K. Chaudhari, Physicochemical treatment of distillery wastewater—a review, Chem. Eng. Commun., 202 (2015) 1098–1117.